




uHD: Unary Processing for Lightweight and Dynamic Hyperdimensional Computing

Sercan Aygun , Mehran Shoushtari Moghadam , M. Hassan Najafi 

School of Computing and Informatics, University of Louisiana at Lafayette, LA, USA

{sercan.aygun, m.moghadam, najafi}@louisiana.edu

Abstract—Hyperdimensional computing (HDC) is a novel computational paradigm that operates on long-dimensional vectors known as hypervectors. The hypervectors are constructed as long bit-streams and form the basic building blocks of HDC systems. In HDC, hypervectors are generated from scalar values without taking their bit significance into consideration. HDC has been shown to be efficient and robust in various data processing applications, including computer vision tasks. To construct HDC models for vision applications, the current state-of-the-art practice utilizes two parameters for data encoding: pixel intensity and pixel position. However, the intensity and position information embedded in high-dimensional vectors are generally not generated dynamically in the HDC models. Consequently, the optimal design of hypervectors with high model accuracy requires powerful computing platforms for training. A more efficient approach to generating hypervectors is to create them *dynamically* during the training phase, which results in accurate, low-cost, and highly performable vectors. To this aim, we use *low-discrepancy* sequences to generate intensity hypervectors only, while avoiding position hypervectors. By doing so, the multiplication step in vector encoding is eliminated, resulting in a power-efficient HDC system. For the first time in the literature, our proposed approach employs lightweight vector generators utilizing *unary bit-streams* for efficient encoding of data instead of using conventional comparator-based generators.

I. INTRODUCTION

Traditional computing systems based on positional binary radix encounter practical limitations in the efficient hardware design of today’s big data applications. Particularly for cognitive tasks with iterative and complex learning procedures, these systems suffer from extremely high power and memory consumption. Emerging computing technologies such as Hyperdimensional Computing (HDC), Stochastic Computing (SC), Unary Bit-stream Computing (UBC), Quantum Computing (QC), and Approximate Computing (AC) are shaping the next generation of computing systems. Among these, HDC has recently gained significant attention due to its lightweight, robust, and efficient solutions for various learning and cognitive tasks [1], [2], particularly for natural language processing [3] and image classification [4]. HDC encodes information using holographic hyperdimensional vectors, known as *hypervectors*, consisting of randomly distributed binary values of -1 (logic-0) and $+1$ (logic-1). This unconventional representation enables fast, robust, efficient, and fully parallel processing of large sets of data [5].

For high-quality HDC, hypervectors are expected to be *orthogonal*, i.e., uncorrelated with each other. By generating *pseudo-random* vectors, prior works encode data to hypervectors that are only *nearly* orthogonal. This work introduces

a novel hypervector encoding scheme, which is radically different from the encoding methods currently used in HDC systems. We propose a simpler and more effective method to achieve orthogonality by drawing an analogy between HDC and SC [6]. Instead of relying on pseudo-randomness, we leverage *quasi-randomness* provided with low-discrepancy (LD) sequences [7] for generating high-quality hypervectors. In addition, for the first time to the best of our knowledge, we take advantage of UBC and its unary data representation [8] for lightweight design of HDC systems. In what follows, we summarize the primary contributions of this work.

- ① Utilizing quantized LD sequences for hypervector encoding for the first time in the literature.
- ② Eliminating position hypervectors in HDC system, alleviating the total memory consumption, vector generation load, and arithmetic operations.
- ③ Developing **uHD**, a hybrid HDC system integrating unary bit-streams and hypervector processing.
- ④ Developing a lightweight combinational logic to compare unary bit-streams for dynamic generation of hypervectors.
- ⑤ A new circuitry for the binarization operation needed in HDC systems.
- ⑥ Achieving a higher image classification accuracy compared to the baseline HDC with pseudo-random hypervectors.

II. BACKGROUND AND MOTIVATION

HDC maps raw input data into a high-dimensional space with hypervectors of $+1$ s and -1 s [9]. Each dimension in this space corresponds to a feature or attribute in the original data. HDC consists of two primary steps: hypervector *generation* and *encoding*, of which the latter creates another hypervector. While the encoding step has been extensively discussed in the literature [2], [10], vector generation is typically left to the performance of pseudo-randomness [11]. When a **scalar** value X is to be represented using a hypervector, its numerical value can be used for vector generation. However, when X is a **symbolic** data, (e.g., a *letter*) a *proper* vector should be attributed to the symbol. The term *proper* emphasizes the importance of orthogonality, as each symbol without numerical information should be treated equally and embedded in hypervectors without any bias towards one symbol over another. In other words, each hypervector should have an equal number of $+1$ s and -1 s with an independent random distribution. This representation requires a good randomness to ensure hypervectors remain uncorrelated with each other. An important target of this work is to produce hypervectors with

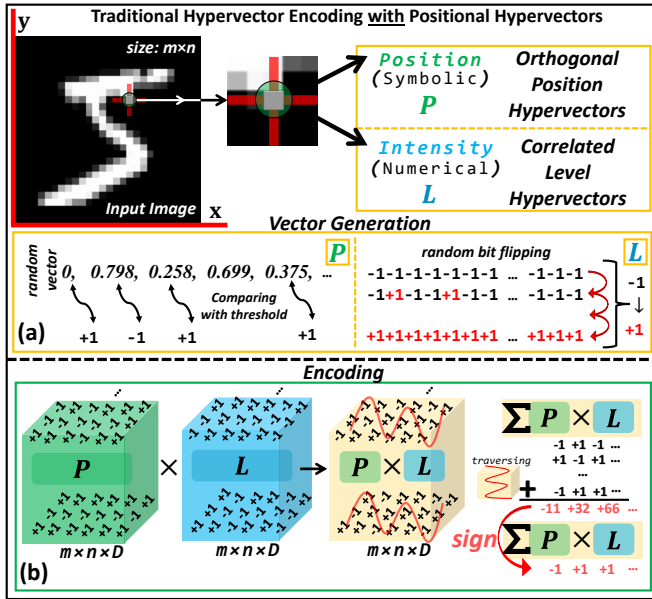


Fig. 1. Traditional hypervector design and encoding. (a) Positional and Level hypervector generation, (b) Binding, Bundling, and Binarization.

ideal orthogonality. For the scalar case, X can be a grayscale pixel value [4] ($0 \leq X \leq 255$ for 8-bit representation), the amplitude of a discrete signal [2], or a numerical feature of data [9]. This work will follow the convention for image classification, so we assume X is a pixel value.

Fig. 1(a) shows a sample image pixel and its position (P) and level (L) hypervectors. Hypervectors are assigned with a dimension or size of D . P s are obtained from **symbolic** data, and L s from **scalar** values. P s are generated by comparing random (R) numbers ($0 \leq R_{1..D} \leq 1$) and a threshold value ($t = 0.5$; *no-bias* point between 0 and 1). L s are typically generated by *bit flipping* [11]. Similar to comparing $t = 0.5$ and random numbers, $0 \leq R \leq D$, each R and threshold $t = k \times \frac{D}{2^n}$ are compared to generate one dimension of L at the k^{th} cycle, where $D \geq 2^n$ (n -bit precision, $k_{max}=2^n$). Hence, closer numerical scalars have similar hypervectors, while different numerical scalars have more uncorrelated hypervectors. In generating both P and L , the comparison returns a +1 or -1 value for any hypervector position. If $R > t$, the corresponding position is set to -1; otherwise, it is set to +1 [2].

Fig. 1(b) illustrates the remaining encoding steps on the generated hypervectors. This step composes the class hypervector (C), which holds the overall representation of a class (e.g., Fig. 1 shows an image from class-5 and its contribution to the corresponding class hypervector). Each image in the training set contributes to building the class hypervectors by processing the hypervectors (P and L) of all its pixels. The generated hypervectors are first multiplied element-wise (via bit-wise XOR). This is known as *binding*. To accumulate the multiplied hypervectors coming from each pixel ($L \oplus P$), positions are traversed. Hypervectors are added to each other by another element-wise processing (bit-wise popcount). This is known as *bundling* [12]. Then, the final values are evaluated for class hypervectors after scanning all data samples of the same class. Finally,

the *binarization* operation is performed via a sign function (thresholding with a comparator or a subtractor) [3]. For each class in training, the labeled data are processed to build its corresponding class hypervector. This operation is performed only once, different from the conventional learning systems having iterative forward passes throughout the batches and epochs.

When all class hypervectors are defined ($C_{1..q}$ with q -class dataset), the inference step measures the accuracy of the testing dataset. The same encoding steps are followed for any testing data to obtain a testing hypervector (C_{test}). The final classification is performed using a similarity check between C_{test} vs. C_1, C_2, \dots , and C_q . In this work, we use cosine similarity. The highest similarity between C_{test} and one of the trained classes gives the classification decision [3].

Generating pseudo-random hypervectors with high orthogonality during training can be very time- and memory-consuming. To obtain a high classification accuracy, the best performing P and L random hypervectors are assigned iteratively. Hypervectors with different distributions are generated iteratively to find those with the highest orthogonality. One of our goals in this work is to minimize the number of vector operations. The bit-wise XOR operations in the binding process involve both P and L hypervectors. We use an encoding for level hypervectors that does not need iteration and provides accurate encoding deterministically [13]. Instead of pseudo-randomness, we provide high orthogonality via *quasi-randomness* ①. Our approach eliminates the need for position encoding and their corresponding multiplications ②. Thus, single-iteration vector optimization is guaranteed thanks to the properties of LD sequences [14].

As the first work of its kind, we use *unary bit-streams* in HDC systems ③. UBC utilizes unary (aka thermometer) coding to represent data using bit-streams with logic-1s (or logic-0s) aligned to the beginning or end of the bit-stream. For instance, $\frac{X_1}{X_2} \Rightarrow \frac{0000011}{0011111}$ are two unary bit-streams of size $N=7$ representing 2 and 5. UBC can be exploited for lightweight design of HDC systems. Hypervector generation in current HDC systems requires conventional binary comparators, which is complex and consumes significant power. We employ UBC to design a new lightweight comparator logic for dynamic hypervector generation ④.

After optimizing vector generation and minimizing the operations in encoding, we also improve the hardware design for the final stage with accumulation and binarization. We propose a concurrent binarization during popcounting; Processing over binary data allows using popcount to only count the number of logic-1s. The binary output is obtained after D cycles to be compared or subtracted from a *threshold* value. This requires a separate module for thresholding or subtraction. We simplify the binarization module to make the decision on the spot while performing popcount ⑤.

III. EFFICIENT HYPERVECTOR ENCODING WITH **uHD**

We call the new unary HDC system **uHD**. **uHD** enjoys a lightweight architecture by taking advantage of unary processing. It also provides a higher accuracy by exploiting the uncorrelation and recurrence properties of LD sequences.

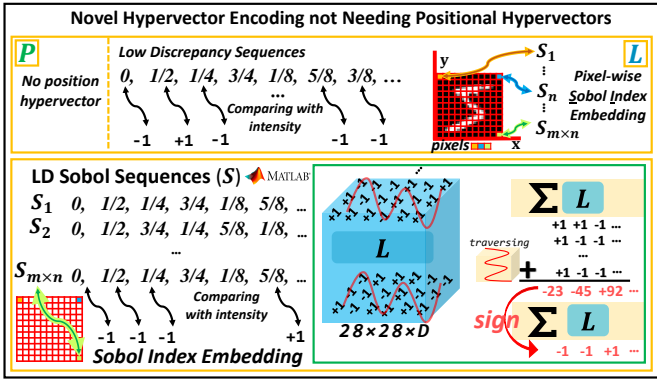


Fig. 2. Hypervector generation using Sobol sequences [15].

uHD radically alters the encoding approach in HDC systems. Conventional HDC systems are bounded by the spatial information of discrete data. LD sequences provide built-in indexes to be used for the positional information. Fig. 2 depicts the encoding using LD Sobol [7] scalars and indexes. We eliminate P_s and only encode L_s by using Sobol scalars. As shown in Fig. 2, for image data encoding, we compare LD Sobol sequences (S_i) (from MATLAB built-in Sobol generator) with image intensity values. We do not encode positions; instead, we use the corresponding index of any Sobol sequence (S_i) ranging from S_1 to $S_{\text{row} \times \text{column}}$. Finally, the non-binary image hypervector formula turns into $\sum_{i=1}^N (L_i)$. Any pixel intensity is encoded based on the pixel position corresponding to the Sobol index. The normalized intensity value (by D) is compared with each element in the corresponding Sobol sequence. If the normalized intensity is smaller than the Sobol number, the hypervector position gets -1 ; otherwise, it gets $+1$. After obtaining L , we perform the accumulation without the encoding's multiplication step. Thus, our novel approach achieves a *multiplier-less* vector encoding for HDC.

Table I compares the performance of the proposed and the baseline HDC with software simulation on an ARM-based embedded processor. We run the low-level C language implementation of the two architectures on a resource-constrained ARM1176JZF-S (700 MHz, 32-bit single core, 250 MB RAM). We compare the two designs in terms of *runtime*, *dynamic memory footprint*, and *code size in memory* for processing each input image. The processing runtime of a single image reduces to 0.016 sec for $D = 1K$ (1024), and to 0.058 sec for $D = 8K$, yielding 43.8 \times and 102.3 \times speed-up, respectively. In terms of dynamic memory allocation, the new encoding scheme using Sobol LD sequences exhibits 10.4 \times less memory for 1K-long and 23.6 \times less memory for $D = 8K$ hypervectors. The memory usage was reduced by 5 KB with the deployed code of the proposed HDC system.

From efficient hypervector design to complete hardware modules, we focus on the extended design perspectives for efficient HDC system design. Most prior works present hardware design for the inference. However, training on edge devices is a more challenging task. Since for high accuracy, the baseline HDC requires iterative hypervector generation and processing, single-pass data processing can significantly

TABLE I
PERFORMANCE ON AN ARM-BASED EMBEDDED PLATFORM [15]

	Performance - Embed.		Runtime	Dyn. Mem.	Code Mem.
	Baseline HDC	Our proposal			Baseline
1K	Baseline HDC	0.701 sec	8,496 KB		13.2 KB
	Our proposal	0.016 sec	816 KB		Ours
8K	Baseline HDC	5.938 sec	52,401 KB		8.2 KB
	Our proposal	0.058 sec	2,220 KB		

reduce the runtime and energy consumption. Our proposed hypervector encoding achieves this benefit with a deterministic and reliable one-time iteration.

uHD reads two sets of data from memory: (i) *processing data* such as image pixels or features and (ii) *Sobol sequences*. In the proposed approach, we quantize both input data and Sobol scalar values. Using Sobol scalar and index encoding removes the need for P_s and corresponding multiplications. We further utilize unary bit-streams instead of the conventional binary radix encoding, bringing UBC into HDC systems for the first time. Now, let us take a look at the overall design. With M -bit quantization, only M -bit data is saved in memory. The input data size depends on the *features* or *raw data* size, such as image's `row` \times `column`. Each Sobol sequence has a length of D (i.e., has D Sobol numbers), where D is typically in the range of 1K to 10K. Storing all Sobol data in registers may not be possible as they may exceed the memory size of the resource-constrained devices. Therefore, we use block RAM (BRAM) in a re-configurable design platform to store the quantized Sobol data. The processing data are relatively lighter in size, so we keep them in registers. Fig. 3(a) illustrates how we keep the data. The data are in quantized binary format (e.g., $M=4$) in registers (REGS). For Sobol scalars, a BRAM module holds binary values in $M=4$ -bit (holding $N=16$ -bit unary bit-streams. Each scalar shows the total count of logic 1s in the stream). An example of quantizing Sobol sequences is shown in Fig. 3(a). Here, $\xi=16$ -level quantization is applied to obtain the to-be-saved binary values. We note that this data quantization does not affect the accuracy of the system. Even though hypervector generation may experience some flipped bits ($+1$ instead of -1 , or vice versa), the accumulated values yield large scalars (non-quantized class hypervector), and the sign of accumulation is not easily affected.

Let us now discuss how we convert the data to unary bit-streams. Unary bit-streams are conventionally generated by using a pair of M -bit binary counter and comparator [16] as shown in Fig. 3(b). This design is compact, especially for dynamic bit-stream generation with large sizes. However, our HDC design works only on $N=16$ -bit sequences, and all possible sequences can be saved in memory. The data in memory are converted to unary bit-streams on-the-fly. Fig. 3(c) shows how we fetch the pre-stored unary bit-streams from an associative memory. The binary scalar in REGS or BRAM points to the corresponding index of a Unary Stream Table (UST), and the target bit-stream is fetched. We put the first design checkpoint here \bullet and compare energy consumption. We synthesize the designs using Synopsys Design Compiler with a 45-nm cell library. We compare the energy consumption of the two approaches for generating one bit of the hypervector. **uHD**

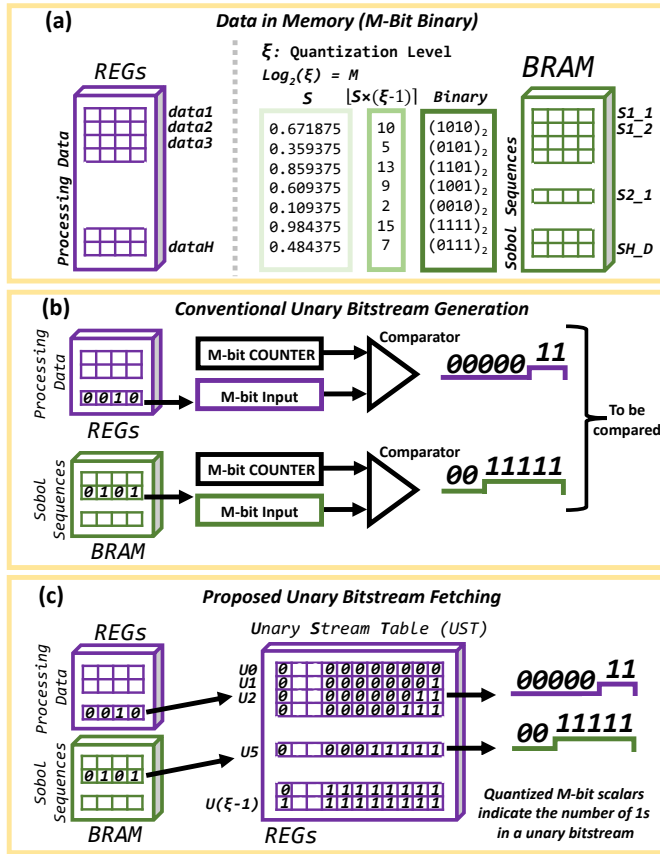


Fig. 3. Getting ready to hypervector generation. (a) Data represented in memory for unary bit-stream processing, (b) Conventional unary stream generation, and (c) proposed associative stream fetching.

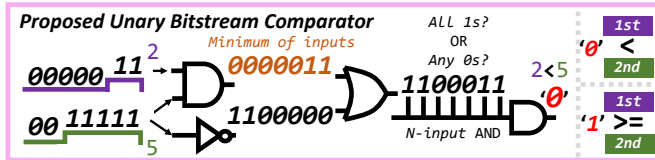


Fig. 4. Proposed comparator of unary bit-streams.

consumes $0.77fJ$ energy while the baseline design consumes $0.167pJ$ (both designed for $D = 1K$).

In our approach, the hypervectors are generated by performing comparison operations between the data and Sobol scalars. Instead of directly comparing quantized scalars via conventional comparators, we use a novel unary bit-stream comparator. Unary bit-streams (with the same length) are correlated, and ANDing them gives the minimum bit-stream. Fig. 4 illustrates the proposed unary comparator for comparing two $N=7$ -bit unary inputs. The data- (■) and Sobol (■) unary bit-streams are compared to generate one bit of the hypervector: If the 1st operand (here, *data*) is greater than or equal to the 2nd operand (here, *Sobol value*), then the corresponding output is logic-1; otherwise, it is logic-0. The bit-wise AND operation determines the *minimum* input. The inverted unary Sobol is checked (by an OR gate) to see if the *minimum* equals this. In the example of Fig. 4, we compare two unary bit-streams corresponding to values 2 and 5. The

minimum (bronze color in Fig. 4) is decided, and the inverted Sobol is checked if bit-wise ORing gives all-1s or at least one logic-0 at the output. If the Sobol number is the *minimum*, the OR operation always returns a logic-1, and ANDing N consecutive bits at the output guarantees a logic-1 bit for the hypervector. If there is at least one logic-0 after OR, the final AND detects it and resets the bit of the hypervector. Since in this example, the data (value of 2 in Fig. 4) is less than the Sobol number (value of 5 in Fig. 4), the output is not all-1s and a logic-0 is generated. Here we have the second design checkpoint ② to evaluate the energy consumption of hypervector generation when using the proposed unary comparator. The baseline HDC with conventional comparators consumes $2.49pJ$, but **uHD** consumes $0.24pJ$ (both designed for $D = 1K$).

When the level hypervectors (L_s) are encoded using the steps above, the next step is the *accumulation* and *binarization*. Fig. 5 illustrates the overall design of **uHD**. The main contributions are underscored in this figure. The red-colored L is traversed for accumulation. For each hypervector bit, a *popcount* operation returns a binary output counting the number of logic-1s. The D-type flip-flops are used in our design for this purpose. We propose a new binarization method that operates concurrently with the *popcount* instead of using an extra subtractor or comparator for the *Threshold of Binarization (TOB)*. The size of the incoming data (the total pixel or feature count), H , is the maximum value to count up. Hence, a $\lceil \log_2 H \rceil$ -bit counter is required. $\frac{H}{2} = TOB$ is the critical threshold reached by *popcount* output for the decision on the logic-1s-in-majority. When the threshold is reached, the sign bit is set for the corresponding bit of the class hypervector; otherwise, it is 0. We propose to use a masking logic for capturing *TOB*, which is in binary: $(B_{\lceil \log_2 H \rceil} \dots B_2 B_1)_2$. As shown in Fig. 5, the masking logic is hardwired, feeding $\lceil \log_2 H \rceil$ bits to the AND gate; When *popcount* reaches *TOB*, this hardwired threshold guarantees logic-1 at the output of AND; otherwise, it remains logic-0 [17]. Here, we set a new design checkpoint ③ and compare the energy consumption of the baseline and **uHD** design for *accumulate-and-binarize* operation. We observe that **uHD** consumes $34.7pJ$ energy per feature of the incoming image, while for the same data the baseline design consumes $68.7pJ$ energy (both designed for $D = 1K$).

IV. DESIGN EVALUATION AND RESULTS

We evaluate the performance, hardware cost, energy consumption, and $\text{area} \times \text{delay}$ of **uHD** compared to the baseline architecture and the prior state-of-the-art (SOTA). We first utilize the standard MNIST dataset for accuracy evaluations [18]. We specifically compare the hardware costs of the baseline and **uHD** architecture for the hypervector generation process. The baseline design follows the dynamic and independent training target. Linear-feedback shift register (LFSR) modules are used for hypervector generation in the baseline design. Table II compares the energy consumption and $\text{area} \times \text{delay}$ product as important metrics to evaluate the hardware efficiency of the proposed design. We note that even though the iterative

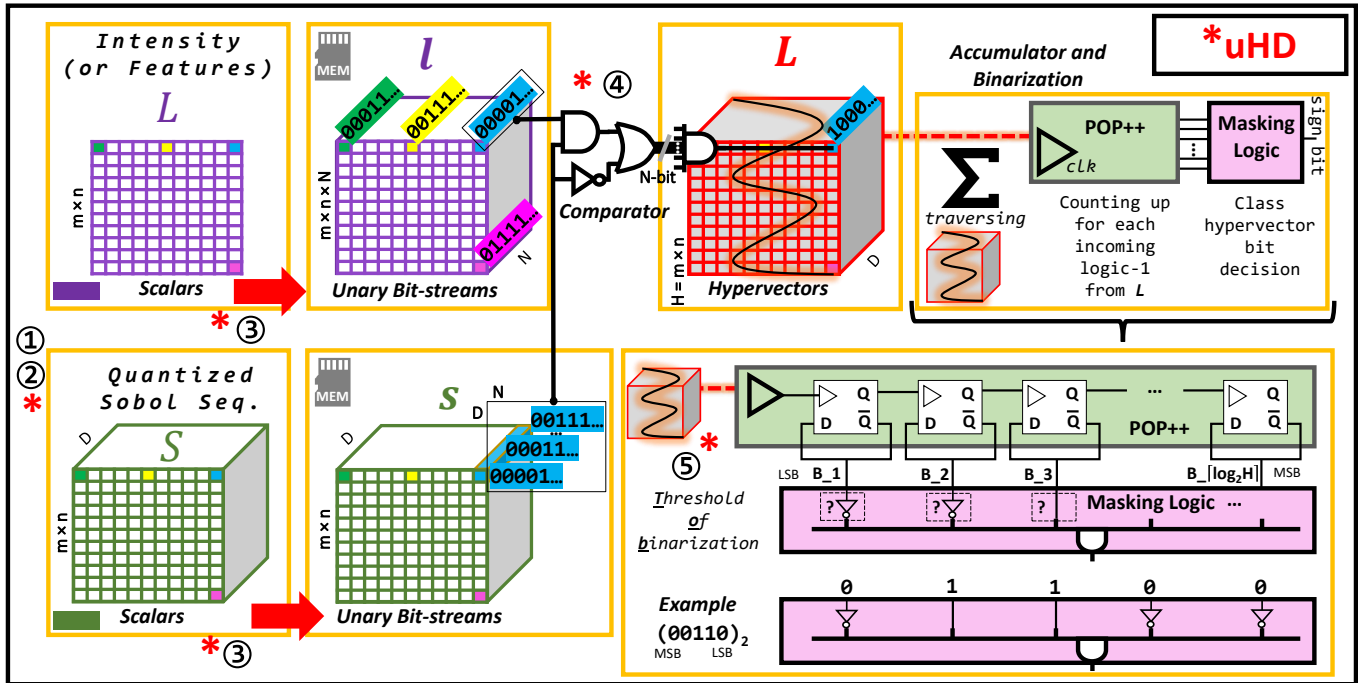


Fig. 5. Complete system overview of **uHD**. * indicates our proposals.

TABLE II
ENERGY CONSUMPTION AND $Area \times Delay$ COMPARISON OF **uHD** AND THE BASELINE HDC FOR EACH HYPERVECTOR (HV) AND IMAGE

Design Approach	Energy Consumption (pJ)			$Area \times Delay$ ($m^2 \times s$)		
	D=1K	D=2K	D=8K	D=1K	D=2K	D=8K
uHD per HV	0.79	1.58	6.32	40.60×10^{-12}	81.20×10^{-12}	324.80×10^{-12}
uHD per image (MNIST)	113.76	227.52	910.08	5.83×10^{-9}	11.67×10^{-9}	46.69×10^{-9}
Baseline per HV	171.42	415.41	4023.82	11.79×10^{-9}	25.55×10^{-9}	230.33×10^{-9}
Baseline per image (MNIST)	24.68×10^3	59.80×10^3	57.94×10^4	1.70×10^{-6}	3.70×10^{-6}	33.17×10^{-6}

design is required for the baseline design (like $i=100$ different attempts to get the best-performing hypervectors), we credit it by assuming that hypervectors are the best, and only a single-run is sufficient for high accuracy. Thus, we provide a fair hardware comparison with respect to **uHD**. However, for a realistic baseline training on an edge device, more iterations are needed for high accuracy, which accordingly increases the energy consumption of the baseline design. We estimate the energy consumption for generating each $P \times L$ hypervector in the baseline HDC (Fig. 1(b)) and for each L hypervector in the **uHD** design (Fig. 2). As can be seen in the reported numbers, our proposed **uHD** is more hardware-efficient than the baseline HDC.

Table III provides a comparative analysis of the SOTA HDC architectures implemented on a central processing unit or microprocessor. A thorough benchmarking is outlined in the HDC surveys by Hassan et al. [19] and Chang et al. [20]. This table ranks the top energy-efficient frameworks for overall architecture (including *hypervector generation*, *binding*, *bundling*, and *binarization*) from the aforementioned surveys and contrasts them with our proposed architecture, which benefits from a novel approach for hypervector generation.

TABLE III
ENERGY EFFICIENCY OVER BASELINE ARCHITECTURES [19], [20]

HDC Framework	Platform	Energy Efficiency
Semi-HD [21]	Raspberry Pi	12.60×
Voice-HD [22]	Central Processing Unit	11.90×
tiny-HD [23]	Microprocessor	11.20×
PULP-HD [24]	ARM Microprocessor	9.9×
Hierarchical-MHD [25]	Central Processing Unit	6.60×
AdaptHD [26]	Raspberry Pi	6.30×
Laelaps [27]	Central Processing Unit	1.40×
This work	ARM Microprocessor	31.83×

In a comprehensive survey conducted in [19] and [20], several HDC frameworks were benchmarked based on their energy efficiency in comparison to reference baseline models. This table lists the top energy-efficient architectures from [19] and [20]. All frameworks, including ours, report the overall (including memory read/write, hypervector generation, binding, and bundling) system energy consumption.

As it can be seen, our proposed HDC architecture provides remarkable energy efficiency by exploiting UBC.

Table IV compares the accuracy performance of the baseline HDC and **uHD**. The baseline architecture is monitored at different iterations of generating hypervectors (P and L). At each random hypervector assignment in the training phase

TABLE IV
MNIST ACCURACY PERFORMANCE (%) OF *Baseline HDC* AND **uHD**

D	Baseline HDC (Average)						uHD
	$i=1$	$i=1..5$	$i=1..20$	$i=1..50$	$i=1..75$	$i=1..100$	$i=1$
1K	82.93	83.60	83.49	82.70	82.88	82.63	84.44
2K	86.24	86.58	87.05	86.35	86.37	86.53	87.04
8K	88.30	88.55	88.25	88.13	88.14	88.13	88.41

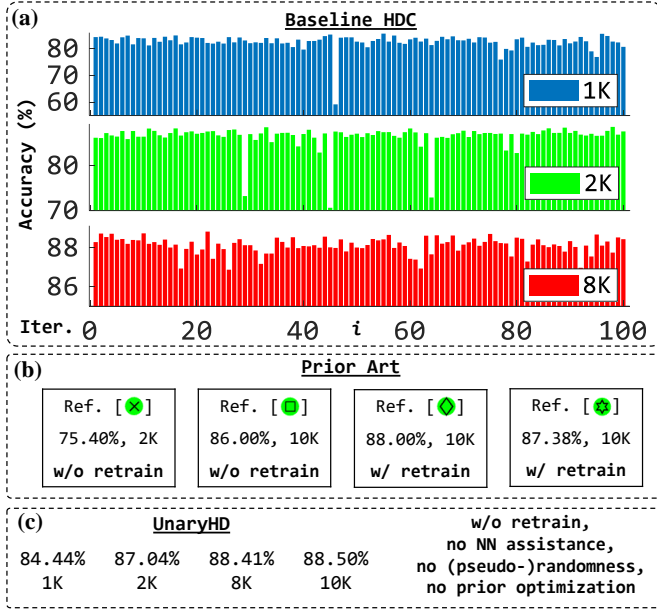


Fig. 6. Different accuracy monitoring of HDC designs. Accuracy fluctuations at each iteration of the baseline design with (pseudo-)randomness (a), MNIST dataset accuracy from prior HDC works; Ref.s $\odot \rightarrow [4]$, $\bullet \rightarrow [19]$, $\odot \rightarrow [28]$, $\odot \rightarrow [9], [29]$ (b), and **uHD** (c).

($i=1..100$), the test accuracy is recorded. The table reports the average accuracy values at different checkpoints of i . **uHD** utilizes LD Sobol sequences and completes its deterministic hypervector (only L) assignment in a single iteration ($i=1$). The MNIST dataset is segmented to separate the training and testing images, and for the sake of fair accuracy comparison between the two designs, there is no retaining, no neural network (NN) assistance, and no prior optimizations. Some prior work heavily relies on these optimizations; however, these optimizations and the use of other machine learning (ML) techniques affect the cost of the training hardware. The impact of using random vectors in the baseline HDC is reported in Fig. 6(a). The fluctuations in the testing accuracy underscore the importance of having an iterative process for selecting the best vectors. Fig. 6(b) reports the accuracy of prior SOTA HDC systems (the ones without NN assistance, complex optimizations in training, or multi-models - only with (w/) or without (w/o) the retraining efforts) in performing MNIST classification. As can be seen, **uHD** with single-pass learning achieves better accuracy compared to the baseline and SOTA designs.

To extend our evaluations, we utilized various image-based datasets, including CIFAR-10, BloodMNIST, BreastMNIST, FashionMNIST, and SVHN [30]. Table V presents the accu-

TABLE V
ACCURACY (%) COMPARISON OF BASELINE HDC AND THE **uHD** FOR DIFFERENT IMAGE DATASETS.

Datasets	D=1K		D=2K		D=8K	
	Ours	Baseline	Ours	Baseline	Ours	Baseline
CIFAR-10	39.29	38.21	40.28	40.26	41.97	41.71
Blood MNIST	53.05	48.52	55.86	51.20	57.88	51.82
Breast MNIST	68.59	68.47	69.23	69.11	71.15	70.93
Fashion MNIST	68.60	54.19	70.06	69.97	71.37	70.87
SVHN	60.29	60.06	61.73	61.24	62.87	62.82

For the Baseline HDC, the P and L hypervectors were generated using conventional random sequence generation.

racy comparison between the baseline HDC and our proposed **uHD**. We note that these accuracy results were obtained without employing any optimization (e.g., retraining, NN assistance, or transfer learning). The findings demonstrate the effectiveness and versatility of **uHD** across different datasets, showcasing its potential for various machine vision applications. The ISO-accuracy values presented above demonstrate that **uHD** exhibits superior hardware efficiency compared to conventional learning frameworks (ML, DNN), which often require resource-intensive hardware setups. As a result, **uHD** offers a more efficient and cost-effective solution to achieve the same accuracy level.

V. CONCLUSIONS

This study proposed a hybrid HDC system, **uHD**, by employing UBC in HDC for the first time. The new design simplifies hardware implementation, providing significant hardware cost savings compared to the baseline HDC. **uHD** utilizes LD sequences for deterministic and high-quality generation of hypervectors. It achieves higher accuracy compared to the baseline HDC while offering single-iteration training. We propose a novel hypervector generator by representing data in the unary domain and comparing data using a novel unary comparator. The impact of adding the proposed modules is studied by comparing the energy consumption of the proposed design with the baseline HDC at different design checkpoints. We hope that this work opens new avenues for HDC by employing the complementary advantages of emerging computing technologies such as SC and UBC.

ACKNOWLEDGMENTS

This work was supported in part by National Science Foundation (NSF) grant #2019511, the Louisiana Board of Regents Support Fund #LEQSF(2020-23)-RD-A-26, and generous gifts from Cisco, Xilinx, and Nvidia.

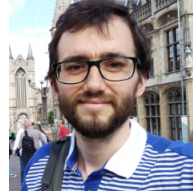
REFERENCES

- [1] S. Aygun, M. S. Moghadam, M. H. Najafi, and M. Imani, "Learning from hypervectors: A survey on hypervector encoding," 2023, arXiv:2308.00685. [Online]. Available: <https://arxiv.org/abs/2308.00685>
- [2] L. Ge and K. K. Parhi, "Classification using hyperdimensional computing: A review," *IEEE Circ. and Syst. Mag.*, vol. 20, no. 2, pp. 30–47, 2020.
- [3] A. Rahimi, P. Kanerva, and J. M. Rabaey, "A robust and energy-efficient classifier using brain-inspired hyperdimensional computing," 2016, p. 64–69.

- [4] S. Datta, R. A. G. Antonio, A. R. S. Ison, and J. M. Rabaey, "A programmable hyper-dimensional processor architecture for human-centric iot," *IEEE JETCAS*, vol. 9, no. 3, pp. 439–452, 2019.
- [5] O. Räsänen *et al.*, "Modeling dependencies in multiple parallel data streams with hyperdimensional computing," *IEEE SPL*, vol. 21, no. 7, 2014.
- [6] A. Alaghi, W. Qian, and J. P. Hayes, "The promise and challenge of stochastic computing," *IEEE TCAD*, vol. 37, no. 8, pp. 1515–1531, 2018.
- [7] S. Liu and J. Han, "Energy efficient stochastic computing with sobol sequences," in *DATE*, 2017, pp. 650–653.
- [8] D. Wu, J. Li, R. Yin, H. Hsiao, Y. Kim, and J. S. Miguel, "Ugemm: Unary computing architecture for gemm applications," in *47th ISCA*, 2020, pp. 377–390.
- [9] M. Imani, S. Bosch, S. Datta, S. Ramakrishna, S. Salamat, J. M. Rabaey, and T. Rosing, "Quanthd: A quantization framework for hyperdimensional computing," *IEEE TCAS*, vol. 39, no. 10, pp. 2268–2278, 2020.
- [10] D. Kleyko, D. A. Rachkovskij, E. Osipov, and A. Rahimi, "A survey on hyperdimensional computing aka vector symbolic architectures, part i: Models and data transformations," *ACM Comput. Surv.*, vol. 55, no. 6, dec 2022. [Online]. Available: <https://doi.org/10.1145/3538531>
- [11] T. Basaklar, Y. Tuncel, S. Y. Narayana, S. Gumussoy, and U. Y. Ogras, "Hypervector design for efficient hyperdimensional computing on edge devices," 2021, arXiv 2103.06709.
- [12] A. Rahimi, P. Kanerva, L. Benini, and J. M. Rabaey, "Efficient biosignal processing using hyperdimensional computing: Network templates for combined learning and classification of exg signals," *Proceedings of the IEEE*, vol. 107, no. 1, pp. 123–143, 2019.
- [13] S. Aygun, M. H. Najafi, and M. Imani, "A linear-time, optimization-free, and edge device-compatible hypervector encoding," in *2023 DATE*, 2023, pp. 1–2.
- [14] S. Liu and J. Han, "Toward energy-efficient stochastic circuits using parallel sobol sequences," *IEEE TVLSI*, vol. 26, no. 7, 2018.
- [15] M. S. Moghadam, S. Aygun, and M. H. Najafi, "No-multiplication deterministic hyperdimensional encoding for resource-constrained devices," *IEEE Embedded Systems Letters*, 2023.
- [16] M. H. Najafi, D. J. Lilja, M. D. Riedel, and K. Bazargan, "Low-cost sorting network circuits using unary processing," *IEEE VLSI*, vol. 26, no. 8, pp. 1471–1480, 2018.
- [17] S. Aygun, E. O. Gunes, and C. De Vleeschouwer, "Efficient and robust bitstream processing in binarised neural networks," *Electronics Letters*, vol. 57, no. 5, pp. 219–222, 2021.
- [18] Y. Lecun, L. Bottou, Y. Bengio, and P. Haffner, "Gradient-based learning applied to document recognition," *Proceedings of the IEEE*, vol. 86, no. 11, pp. 2278–2324, 1998.
- [19] E. Hassan, Y. Halawani, B. Mohammad, and H. Saleh, "Hyperdimensional computing challenges and opportunities for ai applications," *IEEE Access*, vol. 10, pp. 97 651–97 664, 2022.
- [20] C.-Y. Chang, Y.-C. Chuang, C.-T. Huang, and A.-Y. Wu, "Recent progress and development of hyperdimensional computing (hdc) for edge intelligence," *IEEE Journal on Emerging and Selected Topics in Circuits and Systems*, pp. 1–1, 2023.
- [21] M. Imani, S. Bosch, M. Javaheripi, B. Rouhani, X. Wu, F. Koushanfar, and T. Rosing, "Semihd: Semi-supervised learning using hyperdimensional computing," in *ICCAD*, 2019, pp. 1–8.
- [22] M. Imani, D. Kong, A. Rahimi, and T. Rosing, "Voicehd: Hyperdimensional computing for efficient speech recognition," in *IEEE ICRC*, 2017, pp. 1–8.
- [23] B. Khaleghi, H. Xu, J. Morris, and T. S. Rosing, "tiny-hd: Ultra-efficient hyperdimensional computing engine for iot applications," in *DATE*, 2021, pp. 408–413.
- [24] F. Montagna, A. Rahimi, S. Benatti, D. Rossi, and L. Benini, "Pulp-hd: Accelerating brain-inspired high-dimensional computing on a parallel ultra-low power platform," in *DAC*, 2018, pp. 1–6.
- [25] M. Imani, C. Huang, D. Kong, and T. Rosing, "Hierarchical hyperdimensional computing for energy efficient classification," in *DAC*, 2018, pp. 1–6.
- [26] M. Imani, J. Morris, S. Bosch, H. Shu, G. D. Micheli, and T. Rosing, "Adaphd: Adaptive efficient training for brain-inspired hyperdimensional computing," in *BioCAS*, 2019, pp. 1–4.
- [27] A. Burrello, L. Cavigelli, K. Schindler, L. Benini, and A. Rahimi, "Laelaps: An energy-efficient seizure detection algorithm from long-term human i EEG recordings without false alarms," in *DATE*, 2019, pp. 752–757.
- [28] C.-Y. Hsieh, Y.-C. Chuang, and A.-Y. A. Wu, "Fl-hdc: Hyperdimensional computing design for the application of federated learning," in *AICAS*, 2021, pp. 1–5.
- [29] S. Duan, X. Xu, and S. Ren, "A brain-inspired low-dimensional com-

puting classifier for inference on tiny devices," 2022.

- [30] "Datasets," *Hugging Face Datasets*, accessed: Sept. 17, 2023, <https://huggingface.co/datasets?sort=trending>.



Sercan Aygun (S'09-M'22) received a B.Sc. degree in Electrical & Electronics Engineering and a double major in Computer Engineering from Eskisehir Osmangazi University, Turkey, in 2013. He completed his M.Sc. degree in Electronics Engineering from Istanbul Technical University in 2015 and a second M.Sc. degree in Computer Engineering from Anadolu University in 2016. Dr. Aygun received his Ph.D. in Electronics Engineering from Istanbul Technical University in 2022. Dr. Aygun's Ph.D. work has appeared in several Ph.D. Forums of top-tier conferences, such as DAC, DATE, and ESWEEK. He received the Best Scientific Research Award of the ACM SIGBED Student Research Competition (SRC) ESWEEK 2022 and the Best Paper Award at GLSVLSI'23. Dr. Aygun's Ph.D. work was recognized with the Best Scientific Application Ph.D. Award by the Turkish Electronic Manufacturers Association. He is currently a postdoctoral researcher at the University of Louisiana at Lafayette, USA. He works on emerging computing technologies, including stochastic and hyperdimensional computing in computer vision and machine learning.



Mehran Shoushtari Moghadam (S'22) received the B.Sc. degree in Computer Engineering - Hardware and the M.Sc. degree in Computer Engineering - Computer Architecture from the University of Isfahan, Iran, in 2010 and 2016 respectively. He distinguished as one of the top-ranking students during both his B.Sc. and M.Sc. studies. He has more than 10 years of experience as a computer hardware and network specialist in the industry. He is currently a Ph.D. student at the School of Computing and Informatics, Center for Advanced Computer Studies, University of Louisiana at Lafayette, Lafayette, LA, USA. His research interests involve emerging and unconventional computing paradigms, including energy-efficient stochastic computing, real-time and highly-accurate brain-inspired computing, and hardware security.



M. Hassan Najafi (S'15-M'18-SM'23) received the B.Sc. degree in Computer Engineering from the University of Isfahan, Iran, the M.Sc. degree in Computer Architecture from the University of Tehran, Iran, and the Ph.D. degree in Electrical Engineering from the University of Minnesota, Twin Cities, USA, in 2011, 2014, and 2018, respectively. He is currently an Assistant Professor with the School of Computing and Informatics, University of Louisiana, LA, USA. His research interests include stochastic and approximate computing, unary processing, in-memory computing, and hyperdimensional computing. He has authored/co-authored more than 75 peer-reviewed papers and has been granted 5 U.S. patents with more pending. In recognition of his research, he received the 2018 EDAA Outstanding Dissertation Award, the Doctoral Dissertation Fellowship from the University of Minnesota, and the Best Paper Award at the ICCD'17 and GLSVLSI'23. Dr. Najafi has been an editor for the *IEEE Journal on Emerging and Selected Topics in Circuits and Systems*.